

Axion-mediated photon-to-photon transitions in high finesse dielectric resonators

Evangelos Almpanis^{1,*}

¹*Physics Division, National Technical University of Athens,
GR-157 80 Zografou Campus, Athens, Greece*

(Dated: June 6, 2025)

Abstract

Axions are hypothetical particles that could address both the strong charge-parity problem in quantum chromodynamics and the enigmatic nature of dark matter. However, if axions exist, their mass remains unknown, and they are expected to interact very weakly with the electromagnetic field, which explains why they have not been detected yet. This study proposes a way to substantially augment the axion-photon interaction by confining the photons within high-quality-factor dielectric resonators, increasing their intensity and lifetime and thus the possibility of interacting with axions in the background. In view of this, we study resonant axion-mediated photonic transitions in millimeter-sized spherical dielectric resonators, based on fully analytical calculations to the first order in perturbation theory. Such resonators exhibit high lifetime Mie resonances in the microwave part of the spectrum, with a separation that can be tailored with the radius of the sphere to match the expected axion frequency, allowing axion-mediated photonic transitions when particular selection rules are fulfilled. Such transitions are expected to be enhanced by more than ten orders of magnitude in the presence of the resonator, compared to transitions occurring in homogeneous space.

PACS numbers:

I. INTRODUCTION

One of the main mysteries in our current understanding of the physical world is dark matter, which is believed to constitute a significant portion of the total mass of the universe¹⁻⁷. Despite its abundance and crucial role in explaining the structure and formation of the universe, dark matter remains undetected due to its weakly interacting nature. A potential candidate for this is the axion⁸, an elementary particle proposed independently as a solution to the strong charge-parity (\mathcal{CP}) problem in quantum chromodynamics (QCD)⁹. Essentially, this problem revolves around the non-violation of \mathcal{CP} symmetry by the strong nuclear force. This is quantified by a parameter, named θ , which has been measured as zero ($\leq 10^{-10}$) in all experiments¹⁰, suggesting a puzzling *fine-tuning* problem. In order to solve this problem, in the 1970's Roberto Peccei and Helen Quinn proposed a new field, known as the Peccei-Quinn field¹¹, from which the axion particle emerges^{12,13}. Given that the existence of axions offers a promising solution to both the enigmatic nature of dark matter and the strong \mathcal{CP} problem, the research on them is vitally important.

Motivated by the original proposal for axions discussed earlier, the concept was extended beyond the strict framework of QCD, leading to proposals that constitute a broader class of axion-like elementary particles^{8,9,14-22} that serve more general theoretical and observational purposes. The common property of all axion and axion-like particles is that they are bosons that interact very weakly with the electromagnetic field through a mixing between the electric and the magnetic field. Interestingly, such a mixing of the electric and the magnetic field is possible (without the need for cosmic axions) in exotic solid-state materials, so-called magnetoelectric (ME) or Tellegen materials. This class of materials was first conceptually conceived by B. Tellegen²³, while independently, the ME effect (equivalent to Tellegen) was conceptualized by L. Landau²⁴ and predicted in Cr_2O_3 by I. Dzyaloshinskii²⁵, followed by experimental verifications^{26,27}. However, until now, the observed ME phenomena are negligible in most materials with the exception of certain topological insulators, also called *axion insulators*²⁸⁻³³, and more specifically the antiferromagnetically-doped topological insulators, where *axion quasiparticles* can arise due to the intrinsic magnetic properties and the unique structure of the material^{34? -36}.

Now, a possible enhanced coupling between axion quasiparticles (solid state axions) and cosmic axions^{34,35} has generated proposals for a new generation of cosmic axion detectors

named TOORAD (TOpOlogical Resonant Axion Detection)³⁷. We note here that searching for cosmic axions is like tuning a radio: it needs a specific frequency but we don't know what that frequency is (where the role of the frequency is played by the mass of the axion). In this respect, the TOORAD experiment will search for cosmic axions with a mass of 0.7 to 3.5 meV (in natural units), it complements — rather than replaces — more established experimental avenues such as haloscopes and helioscopes. Haloscopes, like ADMX^{38–40}, are designed to detect axions from the Galactic dark matter halo (masses $\sim \mu\text{eV}$) by converting them into photons inside a microwave cavity tuned to the axion mass. More recently, dielectric Haloscopes^{41,42} and plasma Haloscopes^{43–45} have also been proposed. In contrast, helioscopes such as CAST^{46,47} and the next-generation IAXO^{48,49} aim to detect axions produced in the Sun via their conversion into x-rays in a strong magnetic field. Together, these approaches, along with others, cover complementary regions of the axion parameter space.

If QCD axions (pseudoscalar bosons with spin $\mathcal{S} = 0$) exist, they will interact with the photon (vector boson with spin $\mathcal{S} = 1$) in a very specific way. A photon γ_i could absorb an axion α to produce a photon γ_f with increased frequency, i.e. $\gamma_i + \alpha \rightarrow \gamma_f$. Alternatively, a photon γ_i could produce an axion α and a photon γ_f with a lower frequency ($\gamma_i \rightarrow \gamma_f + \alpha$). Such processes involving two photons and one axion⁵⁰ are obviously allowed and can be viewed as axion-mediated transitions from photon γ_i to photon γ_f . We note here that for photons with energies in the $\sim 1\text{meV}$ scale that we will consider in this work, the momentum is on the order of $\sim 1\text{meV}/c$, while the momentum of nonrelativistic dark matter axions (like the ones investigated with Haloscopes⁴¹) is expected to be at the order of $\sim \mu\text{eV}/c$, which is negligibly small compared to that of the photons. In view of this, the axion acts as an energy reservoir, enabling photonic transitions without significant momentum mismatch⁵¹.

Since the axion-photon-photon coupling constant $g_{\alpha\gamma\gamma}$ is very small, here we propose a strategy to significantly enhance the photon intensity and lifetime inside a high quality-factor (Q) dielectric resonator, increasing in this way the probability for axion-photon interactions, when axions with specific mass exist in the background, and particular selection rules are being respected. At first, in Sec. II we define the distinct multipolar eigenstates of the electromagnetic (EM) field inside a spherical dielectric resonator. In Sec. III we come up with the axion-photon interaction expressed through a new term in the Maxwell Lagrangian. In Sec. IV we set up the resonant axion-mediated photonic transitions evaluated to first order in perturbation theory, and establish the selection rules that govern such transitions. This

approach is sufficient for our purposes, while at the same time allowing for a deeper insight into the underlying physics. In Sec. V, which is devoted to the discussion of our results, we provide our fully analytical calculations for the enhancement of the axion-mediated photonic transition rates in the presence of an optical resonator and give specific results. The last section summarizes the main findings of the paper.

II. PHOTONIC RESONANT FREQUENCIES OF A SPHERICAL MIE RESONATOR

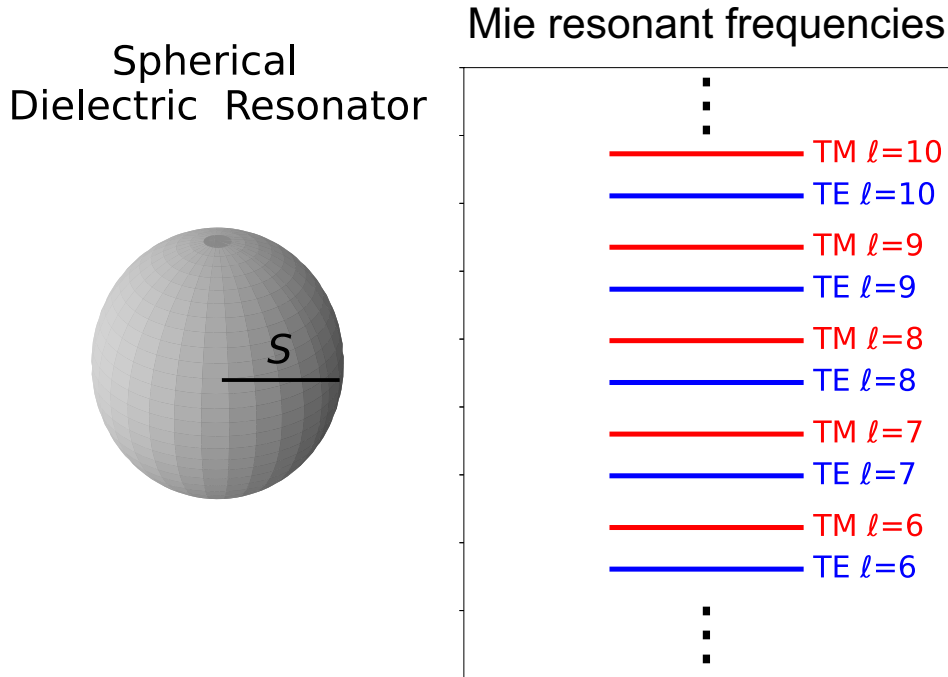


FIG. 1: Discrete photonic Mie resonance frequencies for a spherical dielectric resonator of radius S corresponding to fundamental ($n = 1$) TE (blue) and TM (red) modes of angular momentum ℓ . The dots indicate the presence of additional modes beyond the displayed range.

We will consider a homogeneous and isotropic dielectric sphere (relative permittivity ϵ , relative permeability μ) of radius S in air (free space permittivity ϵ_0 , free space permeability μ_0). Scattering of light by such a sphere can be solved analytically in the framework of Mie theory^{52–54}, assuming a spherical expansion of both incoming and outgoing fields. By doing

so, multiple peaks appear in the corresponding scattering cross section spectrum, the so-called optical Mie resonances. Although these modes have finite lifetime, when the refractive index of the scatterer is high (as in TiO_2 , Si, or Ge) the lifetime is very long, leading to quality factors on the order of $Q \sim 10^3 - 10^6$. Each Mie mode is characterized by the polarization type: magnetic type (TE) or electric type (TM), the angular momentum index ℓ , and the magnetic number m . Throughout this work, we restrict our analysis to fundamental modes with radial index $n = 1$. We note here that due to spherical symmetry, these modes are degenerate ($2\ell + 1$ degeneracy). In Fig. 1 we schematically show the resonance frequencies of the different spectrally separated Mie modes of a spherical dielectric resonator. The electric and magnetic fields, inside the sphere, of a TE mode with resonance frequency ω_1 are given by the expressions^{55–57}

$$\begin{aligned} \mathbf{E}_{M\ell m}(\mathbf{r}; \omega_1) &= a_{M\ell m} j_\ell(q_1 r) \mathbf{X}_{\ell m}(\hat{\mathbf{r}}) \\ \mathbf{B}_{M\ell m}(\mathbf{r}; \omega_1) &= -\frac{i}{\omega_1 \mu_0^2 \mu^2} a_{M\ell m} \nabla \times (j_\ell(q_1 r) \mathbf{X}_{\ell m}(\hat{\mathbf{r}})), \end{aligned} \quad (1)$$

while those of a TM mode with resonance frequency ω_2 are given by the expressions

$$\begin{aligned} \mathbf{E}_{E\ell m}(\mathbf{r}; \omega_2) &= \frac{i}{q_2} a_{E\ell m} \nabla \times (j_\ell(q_2 r) \mathbf{X}_{\ell m}(\hat{\mathbf{r}})) \\ \mathbf{B}_{E\ell m}(\mathbf{r}; \omega_2) &= \frac{\sqrt{\epsilon_0 \epsilon}}{(\mu_0 \mu)^{3/2}} a_{E\ell m} j_\ell(q_2 r) \mathbf{X}_{\ell m}(\hat{\mathbf{r}}), \end{aligned} \quad (2)$$

where $q_{1,2} = \omega_{1,2} \sqrt{\epsilon \mu} / c$, c being the velocity of light in vacuum; j_ℓ are the spherical Bessel functions which are finite everywhere; and $\mathbf{X}_{\ell m}(\hat{\mathbf{r}})$ are the vector spherical harmonics, $\sqrt{\ell(\ell+1)} \mathbf{X}_{\ell m}(\hat{\mathbf{r}}) \equiv -i \mathbf{r} \times \nabla Y_{\ell m}(\hat{\mathbf{r}})$. The expansion coefficients $a_{P\ell m}$, $P = E, M$, have units of electric field (V/m) and are determined by the boundary conditions with respect to the coefficients $a_{P\ell m}^0$ of the incoming field⁵⁷.

The symmetry group of a spherical particle, which involves both proper and improper rotations, is the $O(3)$ Lie group. The character table of the $O(3)$ group is shown in Table I. The subscripts g (gerade) and u (ungerade) denote the parity of the multipole, i.e., g for even parity and u for odd parity. We note here that if we assign the index $P = 1$ for magnetic multipoles (TE) and $P = 2$ for electric multipoles (TM), then the sum $P + \ell$ defines the parity of the Mie mode (even or odd)^{57,58}.

$O(3)$	R_θ	$\mathcal{I}R_\theta$
$D_g^{(\ell=0)}$	1	1
$D_u^{(\ell=0)}$	1	-1
$D_g^{(\ell)}$	$\frac{\sin(2\ell+1)\theta/2}{\sin\theta/2}$	$\frac{\sin(2\ell+1)\theta/2}{\sin\theta/2}$
$D_u^{(\ell)}$	$\frac{\sin(2\ell+1)\theta/2}{\sin\theta/2}$	$-\frac{\sin(2\ell+1)\theta/2}{\sin\theta/2}$

TABLE I: Character table of the $O(3)$ Lie group ($\ell = 1, 2, 3, \dots$). R_θ are rotation operations through an angle θ ($\theta \in [0, \pi]$) about an axis, and \mathcal{I} is the inversion operation.

III. AXION-PHOTON INTERACTION

The interaction between axion and photon is described by an additional term in the Maxwell Lagrangian^{10,50,59,60} (Lagrangian density, units eV/m³)

$$\mathcal{L}_{\alpha\gamma\gamma} = g_{\alpha\gamma\gamma}\alpha(\mathbf{r}, t)\mathbf{E} \cdot \mathbf{B}, \quad (3)$$

where $\alpha(\mathbf{r}, t)$ is the dimensionless axion field and $g_{\alpha\gamma\gamma}$ the axion-photon-photon coupling constant. In the presence of this term, the Maxwell equations, in a linear medium (ϵ, μ) without conventional⁶¹ free sources (the axionic terms now play the role of sources), can be recast as follows^{10,62}

$$\begin{aligned} \nabla \cdot (\epsilon_0\epsilon\mathbf{E}) &= -g_{\alpha\gamma\gamma}\mathbf{B} \cdot \nabla\alpha(\mathbf{r}, t), & \nabla \cdot \mathbf{B} &= 0 \\ \nabla \times \mathbf{E} &= -\frac{\partial\mathbf{B}}{\partial t}, & \nabla \times \left(\frac{1}{\mu_0\mu}\mathbf{B}\right) &= \frac{\partial(\epsilon_0\epsilon\mathbf{E})}{\partial t} - g_{\alpha\gamma\gamma}(\mathbf{E} \times \nabla\alpha(\mathbf{r}, t) - \frac{\partial\alpha(\mathbf{r}, t)}{\partial t}\mathbf{E}) \end{aligned} \quad (4)$$

whereby by setting the following constitutive relations

$$\mathbf{D} = \epsilon_0\epsilon\mathbf{E} + g_{\alpha\gamma\gamma}\alpha(\mathbf{r}, t)\mathbf{B} \quad (5)$$

$$\mathbf{H} = \frac{1}{\mu_0\mu}\mathbf{B} - g_{\alpha\gamma\gamma}\alpha(\mathbf{r}, t)\mathbf{E} \quad (6)$$

we obtain the following set of equations

$$\begin{aligned} \nabla \cdot \mathbf{D} &= 0, & \nabla \cdot \mathbf{B} &= 0 \\ \nabla \times \mathbf{E} &= -\frac{\partial\mathbf{B}}{\partial t}, & \nabla \times \mathbf{H} &= \frac{\partial\mathbf{D}}{\partial t} \end{aligned} \quad (7)$$

Equations (7) are identical to the common Maxwell equations in matter⁶¹ (without free sources). This is analogous to light traveling in an *axionic* medium that mixes the \mathbf{E} and \mathbf{B} fields.

IV. AXION-MEDIATED PHOTONIC TRANSITIONS

In the case of cold dark matter, the axion can be considered as a coherent pseudo-scalar classical field^{34,35,37,63}

$$\alpha(\mathbf{r}, t) = A(\mathbf{r}) \cos \Omega_\alpha t, \quad (8)$$

where $\Omega_\alpha = m_\alpha c^2 / \hbar$ the axion angular frequency and m_α is the axion mass. Since the axionic field varies in time with angular frequency, Ω_α it can induce inelastically scattered light beams with angular frequencies $\omega - \Omega_\alpha$ (Stokes) and $\omega + \Omega_\alpha$ (anti-Stokes), as in typical Brillouin (inelastic) scattering of light by matter excitations^{56,64-68}. In the special case where ω is a resonance frequency of the photonic resonator and $\omega \pm \Omega_\alpha$ is also a (discrete) resonance frequency of the resonator, the so-called (triply) resonant transitions can occur⁶⁹⁻⁷², provided that this is allowed by symmetry (as we shall see later on). We now proceed by modeling this interaction. The constitutive relations (5) and (6) can be cast as a linear system in matrix form as follows

$$\begin{pmatrix} \mathbf{D} \\ \mathbf{H} \end{pmatrix} = \begin{pmatrix} \epsilon_0 \epsilon & g_{\alpha\gamma\gamma} \alpha(t) \\ -g_{\alpha\gamma\gamma} \alpha(t) & \frac{1}{\mu_0 \mu} \end{pmatrix} \begin{pmatrix} \mathbf{E} \\ \mathbf{B} \end{pmatrix} \quad (9)$$

where the 2×2 matrix consists of one static part and one time-dependent part, as follows

$$\begin{pmatrix} \epsilon_0 \epsilon & g_{\alpha\gamma\gamma} \alpha(t) \\ -g_{\alpha\gamma\gamma} \alpha(t) & 1/\mu_0 \mu \end{pmatrix} = \begin{pmatrix} \epsilon_0 \epsilon & 0 \\ 0 & 1/\mu_0 \mu \end{pmatrix} + \begin{pmatrix} 0 & g_{\alpha\gamma\gamma} \alpha(t) \\ -g_{\alpha\gamma\gamma} \alpha(t) & 0 \end{pmatrix} \quad (10)$$

By assuming $\exp(-i\omega t)$ time dependence of the fields, we write the corresponding classical Hamiltonian (energy) density in the following form

$$\begin{aligned}
\mathcal{H} &= \frac{1}{4}(\mathbf{E}^* \cdot \mathbf{D} + \mathbf{B}^* \cdot \mathbf{H}) = \frac{1}{4} \begin{pmatrix} \mathbf{E}^* & \mathbf{B}^* \end{pmatrix} \begin{pmatrix} \mathbf{D} \\ \mathbf{H} \end{pmatrix} \\
&= \frac{1}{4} \begin{pmatrix} \mathbf{E}^* & \mathbf{B}^* \end{pmatrix} \begin{pmatrix} \epsilon_0 \epsilon & 0 \\ 0 & 1/\mu_0 \mu \end{pmatrix} \begin{pmatrix} \mathbf{E} \\ \mathbf{B} \end{pmatrix} + \begin{pmatrix} \mathbf{E}^* & \mathbf{B}^* \end{pmatrix} \frac{g_{\alpha\gamma\gamma}\alpha(t)}{4} \begin{pmatrix} 0 & 1 \\ -1 & 0 \end{pmatrix} \begin{pmatrix} \mathbf{E} \\ \mathbf{B} \end{pmatrix} \\
&\equiv \mathcal{H}_0 + \delta\mathcal{H}(t),
\end{aligned} \tag{11}$$

with the star denoting complex conjugation. The \mathcal{H}_0 is a typical Hamiltonian density for an electromagnetic wave traveling in a linear medium⁶¹ having relative permittivity ϵ and relative permeability μ (unperturbed Hamiltonian), while the term $\delta\mathcal{H}(t)$ that contains all the *axionic* information can be considered as a small time-dependent perturbation. The axion-mediated photonic transitions arise from this dynamical perturbation of the system.

Since the axion-photon coupling is very weak, we can apply the Born approximation up to the first order to calculate the transition amplitudes. In view of this, the useful information is provided by the overlap integral G (transition matrix element), where the perturbation matrix $\delta\hat{V}(t)$ is sandwiched between the final and initial states, i.e, $G = \langle f | \delta\hat{V}(t) | i \rangle$, where

$$|i\rangle = \begin{pmatrix} \mathbf{E}_i \\ \mathbf{B}_i \end{pmatrix} e^{-i\omega_i t} \tag{12}$$

$$\langle f | = \begin{pmatrix} \mathbf{E}_f^* & \mathbf{B}_f^* \end{pmatrix} e^{i\omega_f t}, \tag{13}$$

and

$$\delta\hat{V}(t) = g_{\alpha\gamma\gamma} \frac{A(\mathbf{r}) \cos(\Omega_\alpha t)}{4} \begin{pmatrix} 0 & 1 \\ -1 & 0 \end{pmatrix} = \frac{g_{\alpha\gamma\gamma} A(\mathbf{r})}{2} \begin{pmatrix} 0 & 1 \\ -1 & 0 \end{pmatrix} (e^{-i\Omega_\alpha t} + e^{i\Omega_\alpha t}). \tag{14}$$

The overlap integral (transition matrix element) reads

$$G = \pi [\delta(\omega_i - \omega_f + \Omega_\alpha) + \delta(\omega_i - \omega_f - \Omega_\alpha)] g, \tag{15}$$

where

$$g = g_{\alpha\gamma\gamma} \int_V d^3r A(\mathbf{r}) (\mathbf{E}_f^*(\mathbf{r}) \cdot \mathbf{B}_i(\mathbf{r}) - \mathbf{B}_f^*(\mathbf{r}) \cdot \mathbf{E}_i(\mathbf{r})). \tag{16}$$

The δ functions in Eq. 15 express energy conservation in the optical transitions that involve absorption and emission of one axion by a photon. The volume V is taken as the volume of the sphere since the electromagnetic field decays rapidly outside of the resonator.

Now, it is straightforward to show that $\delta\hat{V}$ remains invariant under proper rotations R_θ , while changes sign under inversions (\mathcal{I}) and improper rotations ($\mathcal{I}R_\theta$), since $A(\mathbf{r})$ is a pseudoscalar, i.e., $A(\mathbf{r}) \xrightarrow{E, R_\theta} 1 \cdot A(\mathbf{r})$ and $A(\mathbf{r}) \xrightarrow{\mathcal{I}, \mathcal{I}R_\theta} -1 \cdot A(\mathbf{r})$. Therefore, $\delta\hat{V}$ is an irreducible tensor operator, which has the symmetry of the $D_u^{(\ell=0)}$ irreducible representation of the Lie group $O(3)$. This means that $\delta\hat{V}$ operating on an eigenvector of the $P\ell$ irreducible subspace, transforms according to the relevant direct product representation

$$\begin{aligned} D_u^{(\ell=0)} \otimes D_g^{(\ell)} &= D_u^{(\ell)}, \\ D_u^{(\ell=0)} \otimes D_u^{(\ell)} &= D_g^{(\ell)} \end{aligned} \quad (17)$$

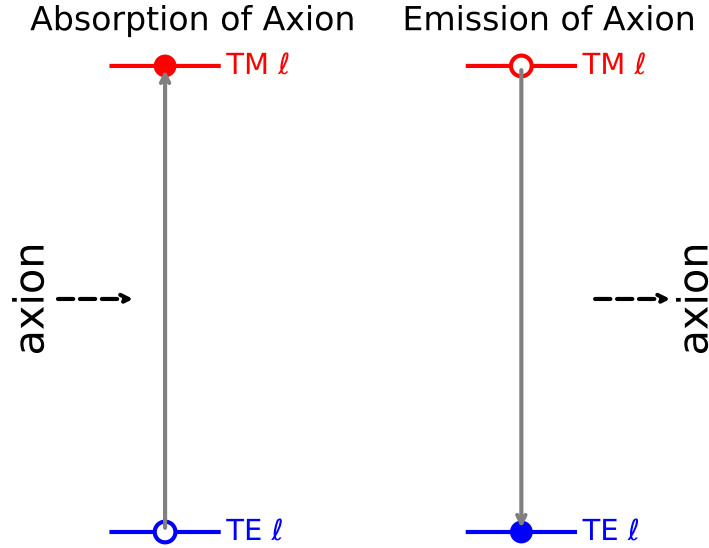


FIG. 2: Schematic representation of axion-induced photonic transitions between electromagnetic modes in a spherical resonator. Left: An axion is absorbed, enabling a transition from a transverse electric (TE) mode to a transverse magnetic (TM) mode with the same angular momentum ℓ . Right: The reverse process, where a transition from TM to TE mode is accompanied by the emission of an axion. The initial and final photonic states are marked with open and solid circles, respectively, while axions are represented by dashed arrows.

These considerations lead to a straightforward selection rule for the photonic transitions described above: the photonic mode must undergo a change in parity, while the angular momentum index ℓ remains conserved, for one-axion absorption (anti-Stokes) and one-axion

emission (Stokes) processes. In Fig. 2 we show a schematic representation of axion-mediated photonic transitions with respect to the mentioned selection rule, provided that the frequency difference of the optical modes is $\Delta f = \Omega_\alpha/2\pi$, where $\Omega_\alpha/2\pi$ is the frequency of the axion. In the left panel we show the anti-Stokes process, where an axion is absorbed by the photonic transition from the TE_ℓ mode with lower frequency to the TM_ℓ mode with higher frequency, while in the right panel we show the inverse process (Stokes) where an axion is emitted by the photonic transition from the TM_ℓ mode with higher energy to the TE_ℓ mode with lower energy. We also note that the same selection rule is deduced by explicitly (analytically) doing the algebra for the $\int \mathbf{E}_{\mathbf{i};P\ell m}^* \cdot \mathbf{B}_{\mathbf{i};P'\ell' m'}$ and $\int \mathbf{B}_{\mathbf{i};P\ell m}^* \cdot \mathbf{E}_{\mathbf{i};P'\ell' m'}$ products and making use of the angular integration properties of the (vector) spherical harmonics.

V. RESULTS AND DISCUSSION

We now assume a spherical lossless high-index dielectric particle of radius S in air. The relative dielectric permittivity of the sphere is $\epsilon = 12$, while its relative magnetic permeability is $\mu = 1$. We will present our results in scaled units of the radius S , nevertheless the radius S can vary from microns to millimeters, depending on the targeted frequency range (we will give specific examples later). As discussed earlier, such particles support long-lifetime, spectrally separated, Mie modes of the EM field, characterized by the indices P and ℓ . Since in such particles the TE_ℓ mode has always lower energy than the corresponding TM_ℓ mode⁵³ (see Fig. 1), as the initial state we set the ℓ multipole of magnetic type (TE) and as the final state we take the ℓ multipole of electric type (TM), for the one-axion absorption process, to comply with the selection rule. The frequency difference between the initial and final states must be adjusted to the axion frequency, $f_f - f_i = \Omega_\alpha/2\pi$, to obtain the resonant transition. We note here that the reverse process (one-axion emission) is also possible, as shown in the right panel of Fig. 2, and the transition matrix element is the same, so will not discuss it for time saving.

In Fig. 3(a) we show the corresponding resonance frequencies for both the TE and TM modes, in scaled units, versus the ℓ index, for ℓ ranging from 6 to 10. Such values of ℓ are typical for high- Q Mie modes. We see an almost linear increase of the Mie mode frequencies with increasing ℓ . In Fig. 3(b) we show the scaled frequency difference $\Delta f S/c$ of modes with the same ℓ . We see that it remains almost constant $\Delta f S/c \simeq 0.05$. This means that

for axion masses at the range of $\sim \mu\text{eV}$ the particle radius would be in the millimeter scale, while the EM radiation will be in the microwave range. Such spherical resonators exhibiting Mie modes can be fabricated and measured experimentally using microwave radiation⁷³.

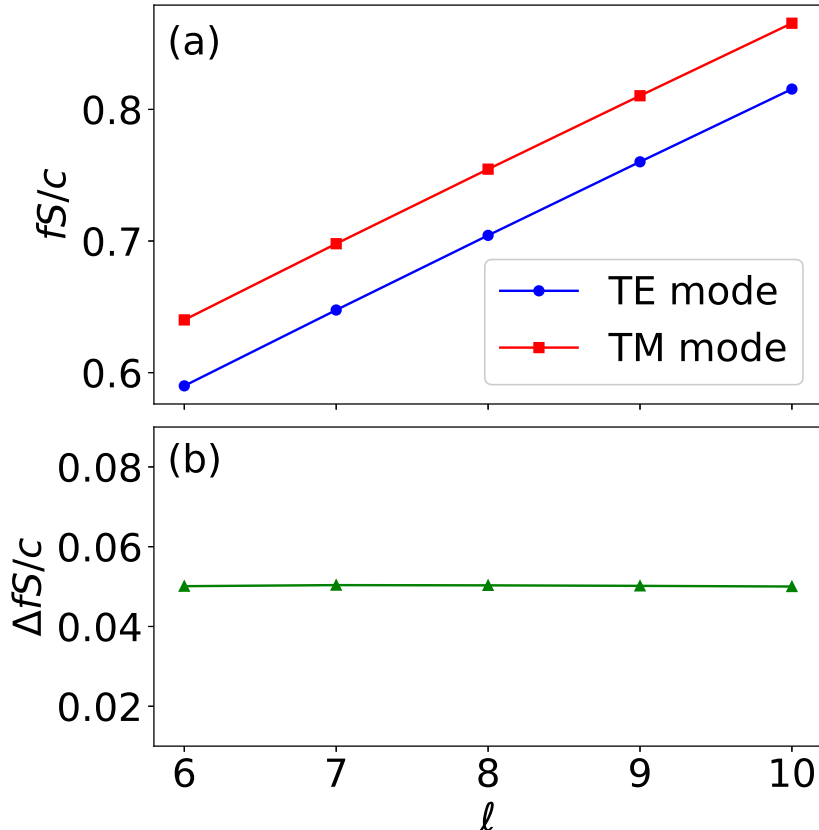


FIG. 3: (a) Scaled eigenfrequencies fS/c for transverse electric (TE) and transverse magnetic (TM) modes of the spherical dielectric resonator under consideration as a function of the angular momentum quantum number ℓ . The data highlights the splitting between TE_ℓ and TM_ℓ modes at each ℓ . (b) The corresponding frequency difference $\Delta fS/c = (f_{\text{TM}_\ell} - f_{\text{TE}_\ell})S/c$, quantifying the frequency difference as a function of ℓ .

Within this range of axion masses and particle radii, we can proceed with the calculation of the respective transition rates. The transition matrix element for one-axion absorption from Eq. 15 (making use of Eqs. 1,2), after some straightforward algebra becomes

$$\begin{aligned}
G &= \frac{\pi g_{\alpha\gamma\gamma}}{2} \int_V d^3r A(\mathbf{r}) (\mathbf{E}_{E\ell m}^*(\mathbf{r}; \omega_f) \cdot \mathbf{B}_{M\ell m}(\mathbf{r}; \omega_i) - \mathbf{B}_{E\ell m}^*(\mathbf{r}; \omega_f) \cdot \mathbf{E}_{M\ell m}(\mathbf{r}; \omega_i)) \\
&= \frac{\pi g_{\alpha\gamma\gamma} A}{2} \sqrt{\epsilon\epsilon_0\mu\mu_0} a_{f;E\ell m}^* a_{i;M\ell m} I(\ell; S, q_i, q_f),
\end{aligned} \tag{18}$$

where $I(\ell; S, q_i, q_f) = \int_0^R \frac{1}{q_i q_f} [(2\ell^2 - \ell + 1 - q_i q_f r^2) j_\ell(q_i r) j_\ell(q_f r) - q_f r(\ell - 1) j_\ell(q_i r) j_{\ell+1}(q_f r) - q_i r(\ell - 1) j_{\ell+1}(q_i r) j_\ell(q_f r) + q_i q_f r^2 j_{\ell+1}(q_i r) j_{\ell+1}(q_f r)] dr$. In Eq. 18 we assumed $A(\mathbf{r})$ to be homogeneous in the volume of the sphere, i.e., $A(\mathbf{r}) \approx A$, since the de Broglie wavelength of the axion is very large (at the order of kilometers³⁷).

The coefficients $a_{i;M\ell m}$, $a_{f;E\ell m}$ can be calculated analytically with respect to an incoming wave with coefficients $a_{i;M\ell m}^0$, $a_{f;E\ell m}^0$, by employing the boundary conditions on the surface of the sphere⁵⁷. In particular, we get

$$a_{i;M\ell m} = W_{M\ell} a_{i;M\ell m}^0, \quad a_{f;E\ell m} = W_{E\ell} a_{f;E\ell m}^0, \tag{19}$$

where

$$\begin{aligned}
W_{M\ell} &= \frac{-i\mu/(q_0 S)}{[x j_\ell(x)]'_{x=q_i S} h_\ell^+(q_0 S) - \mu j_\ell(q_i S) [x h_\ell^+(x)]'_{x=q_0 S}}, \\
W_{E\ell} &= \frac{-i\sqrt{\epsilon\mu}/(q_0 S)}{[x j_\ell(x)]'_{x=q_f S} h_\ell^+(q_0 S) - \epsilon j_\ell(q_f S) [x h_\ell^+(x)]'_{x=q_0 S}},
\end{aligned} \tag{20}$$

where $q_0 = \omega/c$ is the free space wavenumber. Since the coefficients $a_{f;E\ell m}^0$, $a_{i;H\ell m}^0$ describe an EM multipole in free space we can set the transition matrix element in a homogeneous linear medium having relative permittivity ϵ and relative permeability μ as

$$G_0 = \frac{\pi g_{\alpha\gamma\gamma} A}{2} \sqrt{\epsilon\epsilon_0\mu\mu_0} a_{f;E\ell m}^0 a_{i;H\ell m}^0 I(\ell; S, q_i, q_f), \tag{21}$$

Given this, we can calculate the normalized transition matrix element $G/G^0 = W_{M\ell} W_{E\ell}$, from which we can get the enhancement of the transition rate $R_{\alpha\gamma\gamma}$ in the presence of the Mie resonator, versus the transition rate $R_{\alpha\gamma\gamma}^0$ in the homogeneous space (ϵ, μ) , i.e., $R_{\alpha\gamma\gamma}/R_{\alpha\gamma\gamma}^0 = W_{M\ell}^2 W_{E\ell}^2$.

In Fig. 4 we show the relative enhancement $R_{\alpha\gamma\gamma}/R_{\alpha\gamma\gamma}^0$ of the one-axion absorption (emission) rate versus the angular momentum index ℓ . We see that for $\ell = 10$ we obtain a more than ten orders of magnitude enhancement. Such an enhancement can substantially improve the experimental sensitivity to axions in laboratory-scale setups, where the Mie resonator

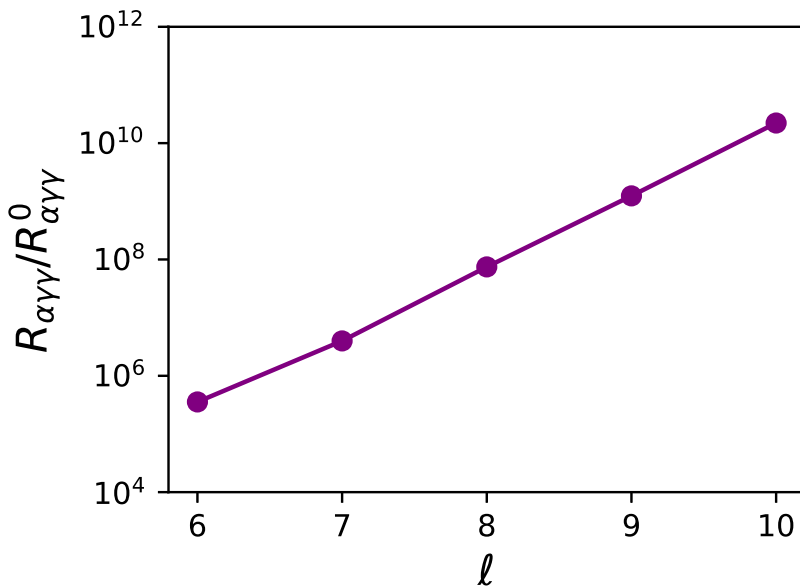


FIG. 4: Enhancement of the axion-mediated photonic transition rate $R_{\alpha\gamma\gamma}$ in the presence of a spherical Mie resonator, plotted as a function of the angular momentum quantum number ℓ . The vertical axis shows the normalized transition rate $R_{\alpha\gamma\gamma}/R_{\alpha\gamma\gamma}^0$, where $R_{\alpha\gamma\gamma}^0$ is the corresponding rate in homogeneous space without the resonator. The plot illustrates in logarithmic scale the resonant enhancement induced by the photonic environment as ℓ increases.

serves as a highly efficient intermediary between the axion field and the photonic environment.

We emphasize that the proposed platform is fully scalable and can be adjusted to the targeted axion mass. Moreover, future investigations could explore whispering-gallery-modes⁷⁴ supported by similar resonators, which are known to exhibit even higher quality factors, thereby enabling further enhancement of the signal. This methodology could also open new directions in searching for axions in mass windows that are inaccessible with the conventional haloscopes and helioscopes. Additionally, our approach might assist the *shining through walls*^{75–78} experiments, where strong laboratory-produced electromagnetic fields could generate axions (through the Primakoff effect) which then pass through opaque barriers and be detected on the far side.

Apart from the (dark matter) axions considered in this work, the underlying mechanism and theoretical framework may also be extended to encompass solid-state ax-

ions (axion quasiparticles). In particular, if the resonator material is chosen to be an antiferromagnetically-doped topological insulator^{34–36} or a bianisotropic^{79–81}/Tellegen metamaterial^{82–87}, it can intrinsically support axion-like electromagnetic responses. Such exotic materials with effective axion electrodynamics are candidates not only for probing fundamental particles but also for engineering dyon-like quasiparticles^{62,88,89}, anyon statistics^{90,91}, effective gauge fields for photons⁹², and accelerating (relativistic) media⁹³, to name a few, *simulating* the physics of fundamental theoretical concepts using solid state media^{94–98}.

VI. CONCLUSIONS

To summarize, we investigated (dark matter) axion-mediated photonic transitions within a spherical, high-finesse dielectric resonator and derived the corresponding selection rule based on group theory. Using the first-order Born approximation, we analytically computed the enhancement of the transition rates associated with one-axion absorption and emission processes. Our results predict a substantial enhancement—exceeding ten orders of magnitude—of the transition rate inside the resonator compared to that in a homogeneous space. These findings could have direct implications for the design of resonant (dark matter) axion devices; moreover, the underlying framework may also inspire future applications in engineered axion-like quasiparticle dynamics in electromagnetic metamaterials.

* e-mail address: ealmpanis@gmail.com

¹ V. C. Rubin and W. K. Ford Jr, *Astrophysical Journal*, vol. 159, p. 379 **159**, 379 (1970).

² S. Heinemeyer, M. Mondragon, and G. Zoupanos, *Journal of High Energy Physics* **2008**, 135 (2008).

³ R. Catena and C. Kouvaris, *Physical Review D* **96**, 063012 (2017).

⁴ N. E. Mavromatos, C. R. Argüelles, R. Ruffini, and J. A. Rueda, *International Journal of Modern Physics D* **26**, 1730007 (2017).

⁵ G. Bertone and D. Hooper, *Reviews of Modern Physics* **90**, 045002 (2018).

⁶ D. F. Jackson Kimball and K. Van Bibber, *The search for ultralight bosonic dark matter* (Springer Nature, 2023).

- ⁷ M. M. Flores, C. Kouvaris, and A. Kusenko, *Physical Review D* **108**, 103545 (2023).
- ⁸ K. Choi, S. H. Im, and C. S. Shin, *Annual Review of Nuclear and Particle Science* **71**, 225 (2021).
- ⁹ J. E. Kim and G. Carosi, *Reviews of Modern Physics* **82**, 557 (2010).
- ¹⁰ C. Adams, N. Aggarwal, A. Agrawal, R. Balafendiev, C. Bartram, M. Baryakhtar, H. Bekker, P. Belov, K. Berggren, A. Berlin, et al., arXiv preprint arXiv:2203.14923 (2022).
- ¹¹ R. D. Peccei and H. R. Quinn, *Physical Review Letters* **38**, 1440 (1977).
- ¹² F. Wilczek, *Physical Review Letters* **40**, 279 (1978).
- ¹³ S. Weinberg, *Physical Review Letters* **40**, 223 (1978).
- ¹⁴ C. Coriano, N. Irges, and S. Morelli, *Journal of High Energy Physics* **2007**, 008 (2007).
- ¹⁵ E. Masso and J. Redondo, *Journal of Cosmology and Astroparticle Physics* **2005**, 015 (2005).
- ¹⁶ A. Chatzistavrakidis, E. Erfani, H. P. Nilles, and I. Zavala, *Journal of cosmology and astroparticle physics* **2012**, 006 (2012).
- ¹⁷ M. D. Marsh, H. R. Russell, A. C. Fabian, B. R. McNamara, P. Nulsen, and C. S. Reynolds, *Journal of Cosmology and Astroparticle Physics* **2017**, 036 (2017).
- ¹⁸ N. E. Mavromatos, *Elementary Particle Physics and Gravity* p. 3 (2017).
- ¹⁹ I. G. Irastorza and J. Redondo, *Progress in Particle and Nuclear Physics* **102**, 89 (2018).
- ²⁰ V. Desjacques, A. Kehagias, and A. Riotto, *Physical Review D* **97**, 023529 (2018).
- ²¹ C. Kouvaris, T. Liu, and K.-F. Lyu, *Physical Review D* **109**, 023008 (2024).
- ²² S. Alexander, T. Manton, and E. McDonough, *Physical Review D* **109**, 116019 (2024).
- ²³ B. D. Tellegen, *Philips Res. Rep* **3**, 81 (1948).
- ²⁴ L. D. Landau and E. M. Lifshits, *Electrodynamics of continuous media*, vol. 2 (Pergamon Press Oxford, 1960).
- ²⁵ I. E. Dzyaloshinskii, *Soviet Physics JETP* **10**, 628 (1960).
- ²⁶ D. Astrov, *Sov. Phys. JETP* **11**, 708 (1960).
- ²⁷ B. Krichevstov, V. Pavlov, R. Pisarev, and V. Gridnev, *Journal of Physics: Condensed Matter* **5**, 8233 (1993).
- ²⁸ L. Wu, M. Salehi, N. Koirala, J. Moon, S. Oh, and N. Armitage, *Science* **354**, 1124 (2016).
- ²⁹ V. Dziom, A. Shuvaev, A. Pimenov, G. Astakhov, C. Ames, K. Bendias, J. Böttcher, G. Tkachov, E. Hankiewicz, C. Brüne, et al., *Nature communications* **8**, 15197 (2017).
- ³⁰ N. Varnava and D. Vanderbilt, *Physical Review B* **98**, 245117 (2018).

- ³¹ D. M. Nenno, C. A. Garcia, J. Gooth, C. Felser, and P. Narang, *Nature Reviews Physics* **2**, 682 (2020).
- ³² A. Sekine and K. Nomura, *Journal of Applied Physics* **129** (2021).
- ³³ T. Z. Seidov and M. A. Gorlach, *Physical Review A* **108**, 053515 (2023).
- ³⁴ D. J. Marsh, K. C. Fong, E. W. Lentz, L. Šmejkal, and M. N. Ali, *Physical Review Letters* **123**, 121601 (2019).
- ³⁵ J. Schütte-Engel, D. J. Marsh, A. J. Millar, A. Sekine, F. Chadha-Day, S. Hoof, M. N. Ali, K. C. Fong, E. Hardy, and L. Šmejkal, *Journal of Cosmology and Astroparticle Physics* **2021**, 066 (2021).
- ³⁶ A. Esposito and S. Pavaskar, *Physical Review D* **108**, L011901 (2023).
- ³⁷ Y. K. Semertzidis and S. Youn, *Science Advances* **8**, eabm9928 (2022).
- ³⁸ T. Nitta, T. Braine, N. Du, M. Guzzetti, C. Hanretty, G. Leum, L. Rosenberg, G. Rybka, J. Sinnis, J. Clarke, et al., *Physical review letters* **131**, 101002 (2023).
- ³⁹ B. T. McAllister, A. P. Quiskamp, and M. E. Tobar, *Physical Review D* **109**, 015013 (2024).
- ⁴⁰ G. Carosi, C. Cisneros, N. Du, S. Durham, N. Robertson, C. Goodman, M. Guzzetti, C. Hanretty, K. Enzian, L. Rosenberg, et al., *arXiv preprint arXiv:2504.07279* (2025).
- ⁴¹ A. J. Millar, G. G. Raffelt, J. Redondo, and F. D. Steffen, *Journal of Cosmology and Astroparticle Physics* **2017**, 061 (2017).
- ⁴² A. Caldwell, G. Dvali, B. Majorovits, A. Millar, G. Raffelt, J. Redondo, O. Reimann, F. Simon, F. Steffen, and M. W. Group), *Physical review letters* **118**, 091801 (2017).
- ⁴³ H. Terças, J. Rodrigues, and J. Mendonça, *Physical Review Letters* **120**, 181803 (2018).
- ⁴⁴ M. Lawson, A. J. Millar, M. Pancaldi, E. Vitagliano, and F. Wilczek, *Physical review letters* **123**, 141802 (2019).
- ⁴⁵ A. J. Millar, S. M. Anlage, R. Balafendiev, P. Belov, K. Van Bibber, J. Conrad, M. Demarteau, A. Droster, K. Dunne, A. G. Rosso, et al., *Physical Review D* **107**, 055013 (2023).
- ⁴⁶ K. Zioutas, S. Andriamonje, V. Arsov, S. Aune, D. Autiero, F. Avignone, K. Barth, A. Belov, B. Beltrán, H. Bräuninger, et al., *Physical review letters* **94**, 121301 (2005).
- ⁴⁷ E. Arik, S. Aune, D. Autiero, K. Barth, A. Belov, B. Beltrán, S. Borghi, G. Bourlis, F. Boydag, H. Bräuninger, et al., *Journal of Cosmology and Astroparticle Physics* **2009**, 008 (2009).
- ⁴⁸ E. Armengaud, F. Avignone, M. Betz, P. Brax, P. Brun, G. Cantatore, J. Carmona, G. Carosi, F. Caspers, S. Caspi, et al., *Journal of Instrumentation* **9**, T05002 (2014).

- ⁴⁹ E. Armengaud, D. Attié, S. Basso, P. Brun, N. Bykovskiy, J. Carmona, J. Castel, S. Cebrián, M. Cicoli, M. Civitani, et al., *Journal of Cosmology and Astroparticle Physics* **2019**, 047 (2019).
- ⁵⁰ G. Galanti and M. Roncadelli, *Universe* **8**, 253 (2022).
- ⁵¹ C. Murgui, Y. Wang, and K. M. Zurek, *Physics Letters B* **855**, 138832 (2024).
- ⁵² G. Mie, *Annalen der physik* **330**, 377 (1908).
- ⁵³ C. F. Bohren and D. R. Huffman, *Absorption and scattering of light by small particles* (John Wiley & Sons, 2008).
- ⁵⁴ J. D. Jackson, *Classical electrodynamics* (John Wiley & Sons, 2021).
- ⁵⁵ N. Stefanou, V. Yannopoulos, and A. Modinos, *Computer physics communications* **113**, 49 (1998).
- ⁵⁶ E. Almpanis, G. Zouros, P. Pantazopoulos, K. Tsakmakidis, N. Papanikolaou, and N. Stefanou, *Physical Review B* **101**, 054412 (2020).
- ⁵⁷ E. Almpanis, G. P. Zouros, and N. Papanikolaou, in *Optomagnonic Structures: Novel Architectures for Simultaneous Control of Light and Spin Waves* (World Scientific, 2021), pp. 243–297.
- ⁵⁸ G. Gantzounis, *The Journal of Physical Chemistry C* **113**, 21560 (2009).
- ⁵⁹ H. S. Røising, B. Fraser, S. M. Griffin, S. Bandyopadhyay, A. Mahabir, S.-W. Cheong, and A. V. Balatsky, *Physical Review Research* **3**, 033236 (2021).
- ⁶⁰ A. Berlin and T. Trickle, *Physical Review Letters* **132**, 181801 (2024).
- ⁶¹ D. J. Griffiths, *Introduction to electrodynamics* (Cambridge University Press, 2023).
- ⁶² F. Wilczek, *Physical review letters* **58**, 1799 (1987).
- ⁶³ S. Chigusa, T. Moroi, and K. Nakayama, *Physical Review D* **101**, 096013 (2020).
- ⁶⁴ C. Wolff, M. Smith, B. Stiller, and C. Poulton, *Journal of the Optical Society of America B* **38**, 1243 (2021).
- ⁶⁵ G. Gantzounis, N. Papanikolaou, and N. Stefanou, *Physical Review B—Condensed Matter and Materials Physics* **84**, 104303 (2011).
- ⁶⁶ E. Almpanis, *Physical Review B* **97**, 184406 (2018).
- ⁶⁷ I. Stefanou, P. A. Pantazopoulos, and N. Stefanou, *Journal of the Optical Society of America B* **38**, 407 (2021).
- ⁶⁸ E. Panagiotidis, E. Almpanis, N. Papanikolaou, and N. Stefanou, *Physical Review A* **106**, 013524 (2022).
- ⁶⁹ J. Haigh, A. Nunnenkamp, A. Ramsay, and A. Ferguson, *Physical review letters* **117**, 133602

- (2016).
- ⁷⁰ X. Zhang, N. Zhu, C.-L. Zou, and H. X. Tang, Physical review letters **117**, 123605 (2016).
- ⁷¹ A. Osada, R. Hisatomi, A. Noguchi, Y. Tabuchi, R. Yamazaki, K. Usami, M. Sadgrove, R. Yalla, M. Nomura, and Y. Nakamura, Physical review letters **116**, 223601 (2016).
- ⁷² E. Panagiotidis, E. Almpanis, N. Papanikolaou, and N. Stefanou, Advanced Optical Materials **11**, 2202812 (2023).
- ⁷³ J.-M. Geffrin, B. García-Cámara, R. Gómez-Medina, P. Albella, L. Froufe-Pérez, C. Eyraud, A. Litman, R. Vaillon, F. González, M. Nieto-Vesperinas, et al., Nature communications **3**, 1171 (2012).
- ⁷⁴ A. Matsko, A. Savchenkov, D. Strekalov, V. Ilchenko, and L. Maleki, IPN Progress Report **42**, 1 (2005).
- ⁷⁵ R. G. Povey, J. G. Hartnett, and M. E. Tobar, Physical Review D—Particles, Fields, Gravitation, and Cosmology **82**, 052003 (2010).
- ⁷⁶ J. Redondo and A. Ringwald, Contemporary Physics **52**, 211 (2011).
- ⁷⁷ S. Gninenko, Physical Review D **89**, 075008 (2014).
- ⁷⁸ A. D. Spector, *Light-Shining-Through-Walls Experiments* (Springer International Publishing, Cham, 2023), pp. 255–279, ISBN 978-3-030-95852-7, URL https://doi.org/10.1007/978-3-030-95852-7_9.
- ⁷⁹ A. Serdyukov, I. Semchenko, S. Tretyakov, and A. Sihvola (2001).
- ⁸⁰ A. Christofi and N. Stefanou, Physical Review B **97**, 125129 (2018).
- ⁸¹ S. F. Koufidis, T. T. Koutserimpas, F. Monticone, and M. W. McCall, Optical Materials Express **14**, 3006 (2024).
- ⁸² F. R. Prudencio, S. A. Matos, and C. R. Paiva, IEEE transactions on microwave theory and techniques **62**, 1417 (2014).
- ⁸³ L. Shaposhnikov, M. Mazanov, D. A. Bobylev, F. Wilczek, and M. A. Gorlach, Physical Review B **108**, 115101 (2023).
- ⁸⁴ S. Safaei Jazi, I. Faniayeu, R. Cicheler, D. C. Tzarouchis, M. M. Asgari, A. Dmitriev, S. Fan, and V. Asadchy, Nature Communications **15**, 1293 (2024).
- ⁸⁵ Q. Yang, X. Wen, Z. Li, O. You, and S. Zhang, Nature Communications **16**, 151 (2025).
- ⁸⁶ T. Z. Seidov and M. A. Gorlach, Physical Review A **111**, 033521 (2025).
- ⁸⁷ S. S. Jazi, I. Faniayeu, R. Cicheler, N. Kuznetsov, S. van Dijken, S. Fan, A. Dmitriev, and

- V. Asadchy, arXiv preprint arXiv:2503.22184 (2025).
- ⁸⁸ X.-L. Qi, R. Li, J. Zang, and S.-C. Zhang, *science* **323**, 1184 (2009).
- ⁸⁹ E. Barredo-Alamilla, D. A. Bobylev, and M. A. Gorlach, *Physical Review B* **109**, 195136 (2024).
- ⁹⁰ I. J. R. Aitchison and N. E. Mavromatos, *Contemporary physics* **32**, 219 (1991).
- ⁹¹ O. Kashuba, R. Mummadaavarapu, and R.-P. Riwar, arXiv preprint arXiv:2410.20835 (2024).
- ⁹² Q. Lin and S. Fan, *Physical Review X* **4**, 031031 (2014).
- ⁹³ F. W. Hehl, Y. N. Obukhov, J.-P. Rivera, and H. Schmid, *The European Physical Journal B* **71**, 321 (2009).
- ⁹⁴ J. Ambjørn, K. Anagnostopoulos, U. Magnea, and G. Thorleifsson, *Nuclear Physics B- Proceedings Supplements* **53**, 725 (1997).
- ⁹⁵ J. Ambjørn, K. Anagnostopoulos, and U. Magnea, *Modern Physics Letters A* **12**, 1605 (1997).
- ⁹⁶ K. Farakos and N. Mavromatos, *Physical Review B* **57**, 3017 (1998).
- ⁹⁷ K. Farakos, G. Koutsoumbas, and N. Mavromatos, *International Journal of Modern Physics B* **12**, 2475 (1998).
- ⁹⁸ A. Paliovaivos, V. Achilleos, G. Theocharis, D. Frantzeskakis, and N. Stefanou, *Physical Review A* **109**, 062229 (2024).